New potential candidates for astronomical searches discovered in the electrical discharge of the PAH naphthalene and acetonitrile

Loru, Donatella; Steber, Amanda L.; Thunnissen, Johannes M.M.; Rap, Daniël B.; Lemmens, Alexander K.; Rijs, Anouk M.; Schnell, Melanie

published in
Journal of Molecular Spectroscopy
2022

DOI (link to publisher)
10.1016/j.jms.2022.111629

document version
Publisher's PDF, also known as Version of record

Journal of Molecular Spectroscopy 386 (2022) 111629

Contents lists available at ScienceDirect

Journal of Molecular Spectroscopy

journal homepage: www.elsevier.com/locate/yjmsp

New potential candidates for astronomical searches discovered in the electrical discharge of the PAH naphthalene and acetonitrile

Donatella Loru [a], Amanda L. Steber [a,1], Johannes M.M. Thunnissen [b], Daniël B. Rap [b], Alexander K. Lemmens [b,c], Anouk M. Rijs [d], Melanie Schnell [a,e,*]

[a] Deutsches Elektronen-Synchrotron DESY, Notkestrasse 85, 22607 Hamburg, Germany
[b] Radboud University, Institute of Molecules and Materials, FELIX Laboratory, Toernooiveld 7c, 6525 ED Nijmegen, the Netherlands
[c] Van't Hoff Institute for Molecular Sciences, University of Amsterdam, Science Park 904, 1098 XH Amsterdam, the Netherlands
[d] Division of BioAnalytical Chemistry, AIMMS Amsterdam Institute of Molecular and Life Sciences, Vrije Universiteit Amsterdam, De Boelelaan 1108, 1081 HV Amsterdam, the Netherlands
[e] Institute of Physical Chemistry, Christian-Albrechts-Universität zu Kiel, Max-Eyth-Straße 1, 24118 Kiel, Germany

ARTICLE INFO

Keywords:
PAHs
Astrochemistry
Plasma chemistry
mid-IR
FELs
Mass spectrometry
IR-UV spectroscopy

ABSTRACT

The formation and dissociation mechanisms of polycyclic aromatic hydrocarbons (PAHs) as well as their reactivity with other interstellar molecules are elusive. In this work, we have investigated the electrical discharge chemistry of the PAH naphthalene and acetonitrile, a molecule known to be present in interstellar environments, using a combination of mass-selective IR-UV ion dip spectroscopy with the free electron laser FELIX in the mid-IR frequency region (550 – 1800 cm^{-1}) and quantum chemical calculations. In addition to the species known to be produced in the electrical discharge of pure naphthalene, $–CH_3$ and –CN substituted unsaturated hydrocarbons have been identified. Most of them, in particular those containing a nitrogen atom in the molecular framework, such as 7H-benzo[7]annulenecarbonitrile, have a substantial dipole moment and, therefore, can be considered as potential candidates for radio astronomical searches. Among the species observed, the two isomers 1- and 2-cyanonaphthalene, which have been recently detected in the TMC-1, have been identified in our experiment, thus continuing to highlight the use of electrical discharge sources as a valuable tool to produce astronomically relevant species.

1. Introduction

The study of molecular infrared emission in the interstellar medium (ISM), designated as the unidentified infrared bands (UIRs), is still under way. Polycyclic aromatic hydrocarbons (PAHs), highly unsaturated carbon molecules composed of two or more fused aromatic rings, have been proposed as the potential carriers of the UIRs, so that they are also referred to as AIBs (Aromatic Infrared Bands). These bands, which are observed in the mid-IR spectral region (roughly from 3 to 20 μm) throughout the interstellar medium (ISM), are characteristic of C–H and C=C stretching and bending vibrational modes of aromatic compounds. Because of the ubiquitous nature of the UIRs, PAHs are considered prominent members of the family of organic molecules in the ISM accounting for about 10 to 25% of the total interstellar carbon [1–3].

Despite the fact that the presence of PAHs has been established, the assignment of individual PAHs to the UIRs via infrared spectroscopy has not yet been possible as only broad IR features have been recorded. The differences in the vibrational frequencies of these C–H and C=C vibrations between several PAHs are smaller than the width of the interstellar band profile, thereby making the disentanglement of these bands difficult. Radio astronomy allows for the unambiguous detection of interstellar molecules; however, in the case of PAHs, the low or even lacking permanent dipole moments as well as their increasing partition functions can make this task challenging or even impossible. Nevertheless, very recently the presence of PAHs in the ISM has been confirmed by the first radio astronomy detections of the PAH indene and of the two carbonitrile-substituted PAHs 1- and 2-cyanonaphthalene in the molecular cloud TMC-1 [4–6]. The detection of the two isomers of cyanonaphthalene is also considered as an indirect detection of the parent hydrocarbon naphthalene.

* Corresponding author.
E-mail address: melanie.schnell@desy.de (M. Schnell).
[1] Current address: Departamento de Química Física y Química Inorgánica, Facultad de Ciencias, Universidad de Valladolid, 47011 Valladolid, Spain.

https://doi.org/10.1016/j.jms.2022.111629
Received 10 December 2021; Received in revised form 13 March 2022; Accepted 8 April 2022
Available online 19 April 2022

Although relevant progress has been made with these detections, the role of PAHs in interstellar environments is still poorly understood. There are open questions with respect to their size distribution, their abundance, their formation, their reactivity, and their potential function as seeds for the formation of larger particles. With regards to their interstellar formation, two models have been proposed. On one side, there is the top-down approach, which is based on the concept that interstellar carbon particles, such as carbon clusters or carbon soot particles, can be destroyed by interstellar UV light to form smaller PAHs [7,8]. Another proposed top-down mechanism explains the formation of PAHs in the ISM through graphene etching on the surface of SiC dust grains [9]. Conversely, there is the bottom-up approach, which postulates that PAHs can form from smaller precursors via chemical reactions. This can occur through gas-phase reactions, such as the hydrogen abstraction-acetylene addition (HACA) mechanism, or via grain-surface reactions [10–13].

To gain insight into the formation of PAHs as well as their reactivity with cyano-containing interstellar molecules in the laboratory, we have used electrical discharge coupled with mass-selective IR-UV ion dip spectroscopy using an infrared free electron laser [14,15]. Under plasma conditions, PAHs are expected to undergo fragmentation processes followed by recombination chemistry. The formed species can be identified via their mass in combination with their characteristic IR features in the 550 – 1800 cm^{-1} fingerprint region. Herein, we present our results obtained from electrical discharge experiments on the PAH naphthalene ($C_{10}H_8$) in mixture with acetonitrile (CH_3CN), a simple nitrogen-containing interstellar molecule and a source of the CN radical, also known to be abundant in several interstellar regions [16–18]. The plasma chemistry of the pure PAH naphthalene has been already investigated using the same experimental technique by Lemmens and coworkers [15]. In that study, new potential reaction pathways for the formation of PAHs were discussed. Carbon insertion resulting in the formation of larger PAHs, namely phenanthrene and pyrene, was observed. Furthermore, that experiment demonstrated that growth of PAHs via the addition of diacetylene units should be taken into consideration, as an alternative to the HACA mechanism.

In the experiment presented here, several new species are observed upon addition of acetonitrile. Among these are the two isomers of cyanonaphthalene, which, as mentioned, have been already detected in the TMC-1. Their observation in our experiment highlights the capability of electrical discharge sources as a powerful laboratory tool, not only to shed light on potential reaction pathways but also to generate new species. The latter could be used as a basis for chemical investigations in TMC-1 and other interstellar clouds and could act as proxies to trace non-polar species via radio astronomy.

2. Experimental and computational methods

The electrical discharge experiment of naphthalene and acetonitrile was performed at the FELIX laboratory using mass-selective IR-UV ion dip spectroscopy coupled with a molecular beam and an electrical discharge source [14,15]. Naphthalene ($C_{10}H_8$, 99% purity) and acetonitrile (CH_3CN, 99.9 % purity) were purchased from Sigma Aldrich and used without further purification. At room temperature, naphthalene is solid with a tabulated melting point of 80 °C. To increase its gas-phase concentration, the sample was heated using a home-built heatable reservoir (to ~ 95 °C), directly connected to a pulsed valve (Parker Series 9 pulse valve) and positioned inside the vacuum chamber. The naphthalene/acetonitrile mixture was created by streaming argon, used as a carrier gas at a backing pressure of ca. 5 bar, first through the reservoir containing acetonitrile external to the vacuum chamber and then through the heatable reservoir containing naphthalene. After exiting the pulsed valve but before supersonic expansion, the gas pulse containing the mixture of the precursors was electrically discharged. The design of the nozzle has been discussed in a previous publication [15] therefore only a brief description is provided here. It consists of two oxygen-free copper electrodes separated by a PEEK spacer and inserted into a PEEK housing. To increase the reaction time between the reactive species and, therefore, to favor the formation of new molecules, a 6 mm spacer was added after the two electrodes forming a recombination zone. To improve the rovibrational cooling after discharge, the final spacer was designed in a way to ensure a compression of the beam before

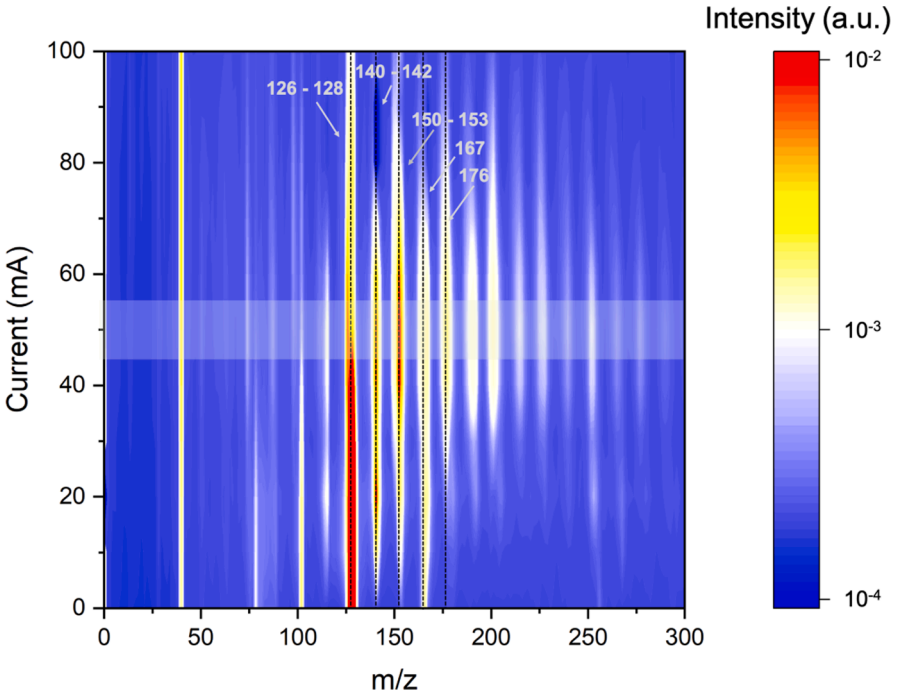

Fig. 1. Discharge current vs. mass-to-charge (m/z) ratio plot showing the range of currents at which the formation of fragments or recombination species is favored. When a current of approximately 50 mA is produced, the intensity of the parent species ($m/z = 128$) decreases, whereas an increase in the intensity of most of the discharge products, as highlighted in the diagram, is observed.

supersonic expansion. For this experiment a voltage between 0.7 and 0.8 kV, which produced a current of about 50 mA, was found to be optimal for the formation of species having a mass-to-charge (m/z) ratio larger than the precursors (Fig. 1).

At the exit of the discharge nozzle the molecular beam, containing a mixture of the carrier gas, the precursors and the newly formed species, was expanded into the vacuum chamber, skimmed and delivered internally cold to the interaction region. Here it was probed using a combination of IR-UV ion dip spectroscopy and mass spectrometry. The formed fragments and products present in the molecular beam were ionized using [1 + 1′] resonant enhanced multiphoton ionization (REMPI) with excitation by a dye laser at 275 nm and ionized with an ArF laser (193 nm). The selection of an excitation wavelength at 275 nm was based on a scan of the laser wavelength for the REMPI process of diacetylenebenzene ($m/z = 126$), which resulted in a broad peak around 275 nm. Excitation wavelengths in the range between 260 and 280 nm are known to enable a selective ionization of (poly)cyclic aromatic species [19], and a fixed excitation wavelength within this range has been previously used in similar experiments [15,20]. At this specific wavelength combination (275 + 193 nm) and laser power, we did not observe any fragmentation of the ions without the electrical discharge. This was verified by recording the mass spectrum of the naphthalene and acetonitrile mixture with and without application of electrical discharge.

The ionized species were then mass-separated and detected using a reflectron time-of-flight mass spectrometer equipped with a multi-channel plate ion detector. For each mass channel, an IR spectrum was recorded in the 550 – 1800 cm^{-1} fingerprint region using the IR-UV ion dip experimental scheme with the free electron laser FEL-2 at the FELIX laboratory [21]. To improve the S/N ratio of the experimental data, several IR spectra (four scans between 550 and 1000 cm^{-1} and three scans between 1000 and 1800 cm^{-1} range) were recorded and averaged together for each mass channel. To better visualize the vibrational features, a 5-point adjacent-average smooth function was applied to the average of the experimental spectra. A comparison between the averaged spectra before and after applying the smooth function is reported in Fig. S1 of the supplementary information.

The assignment of the IR spectra to a specific molecule was achieved by comparing the experimental IR spectra with computed IR spectra of potential candidates. For all indicated mass channels (see Fig. 2), we have optimized the structures of possible isomers with that specific mass and computed their IR spectra. Since the number of possible isomers increases tremendously with increasing mass, the selection of isomers cannot be considered to be comprehensive, but we focused on a broad variety of species selected based on chemical intuition and on results from related experiments. The theoretical spectra were calculated using density functional theory (B3LYP) coupled with the 6–31+G* basis set [22,23] implemented in the Gaussian 16 program [24]. This rather low basis set has been shown to be sufficient for an assignment of the experimental spectra [15]. As the spectra become more complicated for larger masses, NEARIR calculations were performed in order to simulate overtones and combination bands for the molecular species of $m/z = 140$ and 151. For this, calculations using the option NEARIR, which is implemented in the ORCA 5.0 software [25,26], were performed in combination with the B3LYP/def2-TZVP level of theory. The NEARIR calculations provided fundamental bands, combination bands, and overtones. The fundamental bands were individually normalized and the sum of the combination bands with overtones was also individually normalized. Subsequently, these two sets of bands were summed together. The intensity of the theoretical spectra reported here is arbitrary.

A scaling factor of 0.976 and 0.9671 [27] was applied to the

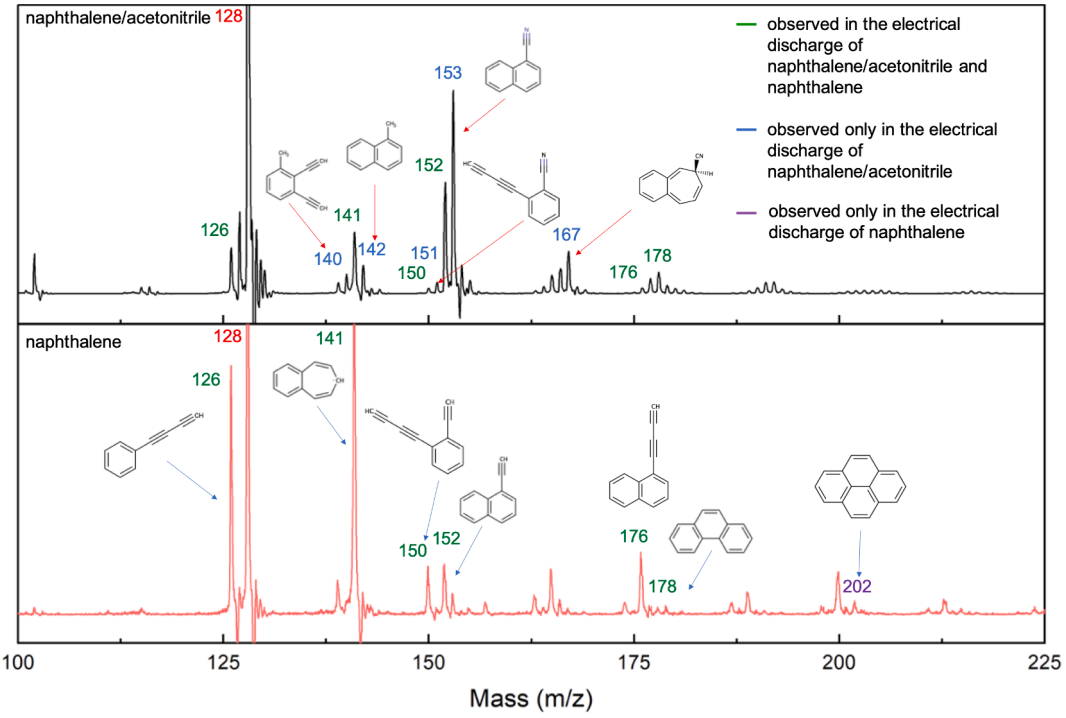

Fig. 2. Comparison of the mass spectra of the products of the electrical discharge of naphthalene and acetonitrile (upper trace in black) and of the electrical discharge of pure naphthalene (lower trace in red) highlighting the similarities and differences in produced species between the two experiments. Both mass spectra were obtained via two-color REMPI (275 nm + 193 nm). The signal at $m/z = 128$, corresponding to the parent species, is truncated in both spectra to improve the visualization of the lower intensity signals. Only the m/z values that are assigned to a specific molecular structure are indicated. The values reported in green, blue, and violet indicate the m/z of species identified in both discharge experiments, only in the discharge experiment of naphthalene and acetonitrile, and only in the discharge experiment of pure naphthalene, respectively. The molecular structure of a representative of the new identified families is also showcased. (For interpretation of the references to color in this figure legend, the reader is referred to the web version of this article.)

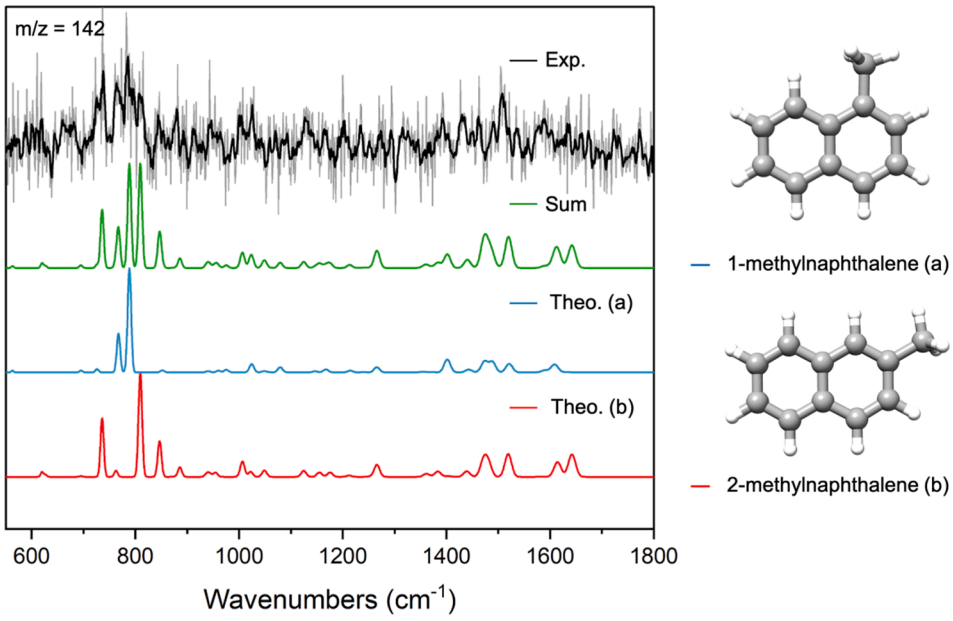

Fig. 3. Comparison of the experimental IR spectrum (black trace) recorded in the 550 – 1800 cm^{-1} region for $m/z = 142$ with the theoretical harmonic vibrational spectra calculated at the B3LYP/6–31+G* level of theory for the two isomers 1-methylnaphthalene (blue trace) and 2-methylnaphthalene (red trace). The trace in light gray represents the average of the experimental IR spectra. The black trace shows the averaged experimental IR spectrum after applying a 5-point adjacent-average smooth function. The green trace provides the sum of the calculated spectra of the two isomers. A scale factor of 0.976 was applied to the theoretical spectra. (For interpretation of the references to color in this figure legend, the reader is referred to the web version of this article.)

frequency scale of the calculated harmonic and NEARIR spectra, which were also convoluted to a Gaussian lineshape function with a full width at half maximum (FWHM) of 1% of the frequency to match the FELIX bandwidth.

3. Results

The products arising from the electrical discharge of pure naphthalene ($m/z = 128$) have been previously investigated using IR-UV mass-selective ion dip spectroscopy [15]. To ease the identification of the new discharge species that form when acetonitrile is added as an additional precursor, we compared the time-of-flight mass spectrum of the discharge of naphthalene and acetonitrile with that of the discharge of pure naphthalene in Fig. 2. Both spectra exhibit peaks at $m/z < 128$ and $m/z > 128$, corresponding to species arising from fragmentation and recombination chemistry, respectively. As expected, there are several peaks in common between the two mass spectra, namely $m/z = 126$, 141, 150, 152, 176, and 178, which were already assigned to specific molecular structures in the discharge of pure naphthalene [15]. The experimental IR spectra of the species in common between the two experiments and their assignments are reported in the supplementary information (Figs. S4-S9). Several new peaks corresponding to $m/z = 140$, 142, 151, 153, and 167 are observed in the mass spectrum with acetonitrile added as a precursor. The two time-of-flight mass spectra also differ in the most prominent discharge product, being $m/z = 153$ and $m/z = 141$ in the electrical discharges of naphthalene and acetonitrile and of pure naphthalene, respectively.

The knowledge of the m/z values is often not sufficient to assign the respective molecular structure, especially those of larger molecules with an increased diversity of possible species, which are more difficult to differentiate. In order to obtain structural information for the different mass channels, spectroscopic information is therefore needed. We have used a combination of mass-selective IR-UV ion-dip spectroscopy in the 550 – 1800 cm^{-1} region and quantum-chemical calculations. The

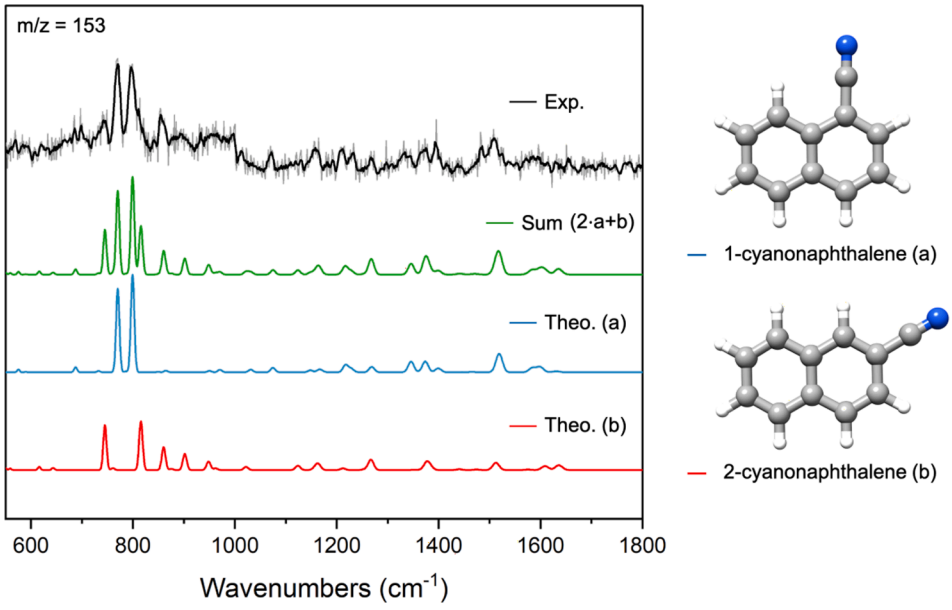

Fig. 4. Comparison of the experimental IR spectrum (black trace) recorded in the 550 – 1800 cm^{-1} frequency region for $m/z = 153$ with the theoretical harmonic vibrational spectra calculated at the B3LYP/6–31+G* level of theory for the two isomers 1-cyanonaphthalene (blue trace) and 2-cyanonaphthalene (red trace). The trace in light gray represents the average of the experimental IR spectra. The black trace shows the averaged experimental IR spectrum after applying a 5-point adjacent-average smooth function. The green trace provides the sum of the calculated spectra of the two isomers. A scale factor of 0.976 was applied to the theoretical spectra. To better match the intensities of the experimental spectrum, the theoretical spectra of 1- and 2-cyanonaphthalene have been combined with a 2:1 ratio, respectively. (For interpretation of the references to color in this figure legend, the reader is referred to the web version of this article.)

assignment was achieved by computing vibrational spectra corresponding to several possible isomers of a certain mass and comparing them with the experimental IR spectrum as shown in Fig. 3 for m/z = 142 and Fig. 4 for m/z = 153. Following our chemical intuition and considering that under electrical discharge conditions acetonitrile is a source of the radicals CN and CH_3 [28], the assignment of m/z = 142 and m/z = 153 to 1- and 2-methylnaphthalene and 1- and 2-cyanonaphthalene, respectively, was straightforward (Fig. 3 and Fig. 4). Note that the relative abundance of the isomers is not reflected in the observed intensity. The latter depends on the excitation and ionization cross section, which can vary depending on the probed molecular species. Furthermore, a quantitative assignment of the observed species cannot be provided since the excitation wavelength was fixed throughout the experiment and not optimized for each mass channel. Both experimental IR spectra corresponding to the mass channels 142 and 153 exhibit vibrational bands in the spectral region between 730 cm^{-1} and 860 cm^{-1}, which are generated by the hydrogen out-of-plane bending motion of substituted aromatic rings. The frequencies of these vibrational bands depend on the position of the substituted aromatic carbon, and this explains the similarities in vibrational frequencies between the vibrational spectra of 1-methylnaphthalene and 1-cyanonaphthalene as well as between the vibrational spectra of 2-methylnaphthalene and 2-cyanonaphthalene. The assignment of 1- and 2-methylnaphthalene and 1-cyanonaphthalene could be further confirmed through comparison of the recorded IR spectra of the present work with that available on the NIST Chemistry WebBook website (see Figs. S2 and S3) [29].

The IR spectrum corresponding to m/z = 140 exhibits a variety of vibrational features along the frequency range investigated (Fig. 5). The presence of an intense vibrational band at ~ 1210 cm^{-1} immediately suggested that at least one of the molecules contributing to the experimental IR spectrum should contain a terminal −C≡C−H group. This band is known to be the result of an overtone generated by the ≡C−H bending motion, and it is considered as a diagnostic band for the identification of −C≡C−H containing structures [30,31]. We have considered a series of isomers containing a −C≡C−H terminal group with a m/z = 140, which are given at the right-hand side of Fig. 5, namely 1-(buta-1,3-diyn-1-yl)-2-methylbenzene (a), 1-(buta-1,3-diyn-1-yl)-3-methylbenzene (b), 1-(buta-1,3-diyn-1-yl)-4-methylbenzene (c), 1,2-diethynyl-3-methylbenzene (d), 1,2-diethynyl-4-methylbenzene (e), 1,3-diethynyl-2-methylbenzene (f), 1,3-diethynyl-5-methylbenzene (g), and 1,3-diethynyl-4-methylbenzene (h). Their vibrational spectra have been calculated and compared with the experimental IR spectrum, as shown

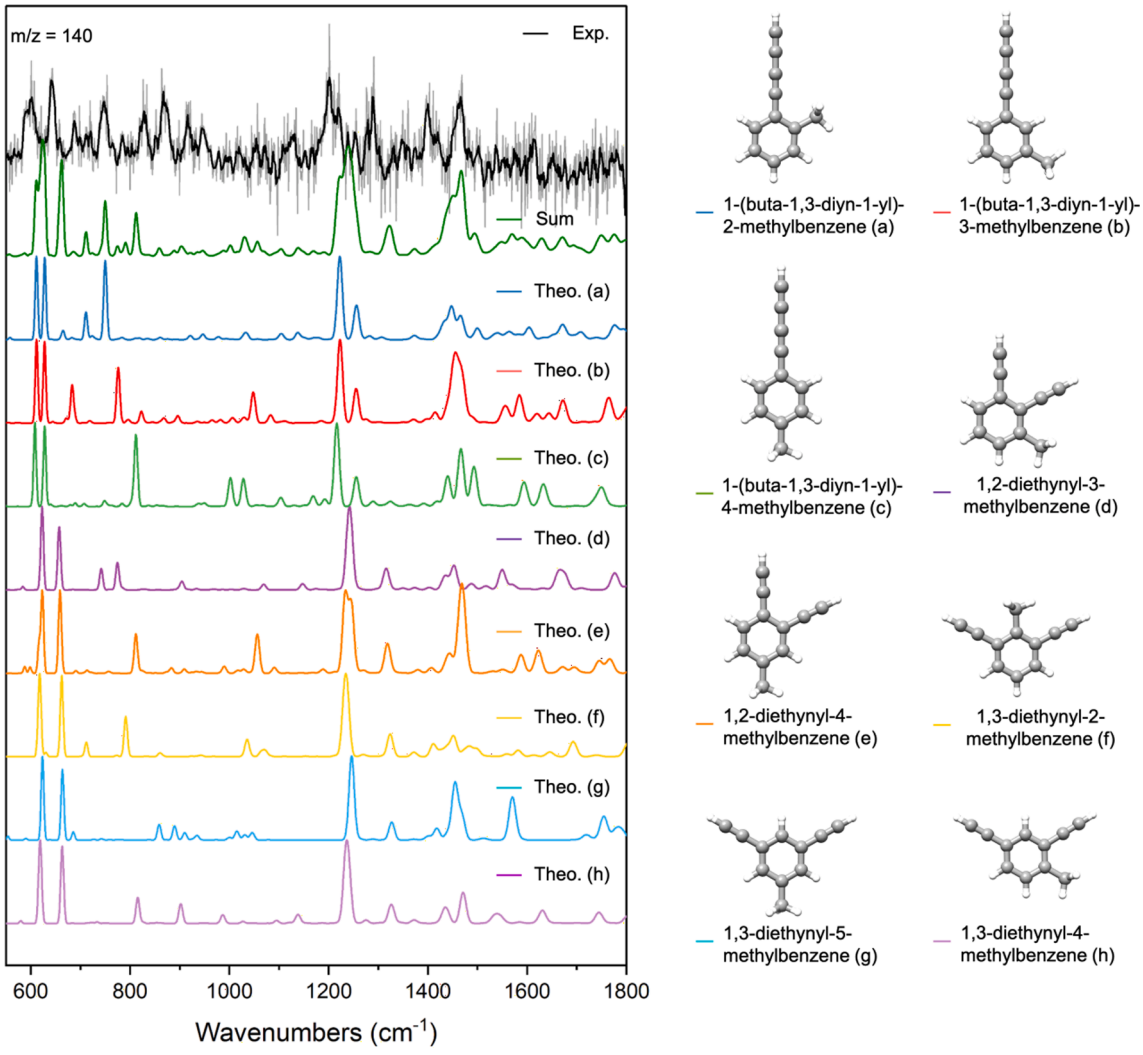

Fig. 5. Comparison of the experimental IR spectrum (black trace) recorded in the 550 – 1800 cm^{-1} frequency region for m/z = 140 with the theoretical NEARIR vibrational spectra calculated at the B3LYP/def2-TZVP level of theory for several isomers (left). The trace in light gray shows the average of the experimental IR spectra. The black trace represents the averaged experimental IR spectrum after applying a 5-point adjacent-average smooth function. The colored traces provide the theoretical vibrational spectra calculated for the molecular structures given on the right-hand side of the figure (a-h). A scale factor of 0.9671 was applied to the theoretical spectra.

in Fig. 5. All of them exhibit a similar vibrational spectrum with the most intense bands falling in the 600 – 800 cm^{-1} region. The combination of their theoretical vibrational spectra with equal weighting, represented by the green trace in Fig. 5, reproduces well the frequency region 600 – 800 cm^{-1}. The bands observed around 600 cm^{-1} arise from the out-of-plane deformation of the −C≡C−H terminal group. These bands are also present in the experimental IR spectra recorded for mass channels 126, 150, and 152, which were assigned to a series of compounds featuring a terminal −C≡C−H group in their molecular structure (Figs. S4, S6, S7, and S8) in the electrical discharge of pure naphthalene. The bands around 750 – 800 cm^{-1} are characteristic of aromatic rings and are generated by the CH out-of-plane bending motion. Those around 1400 cm^{-1} are diagnostic of methyl substituted aromatic rings. However, since most of the isomers show similar vibrational features due to their structural similarities, we cannot ensure that all of them are produced in our discharge experiment and have no detailed information on their relative intensity ratios, so that we used equal weights for the summed theoretical spectrum.

Note that, despite the presence of the −C≡C−H terminal group in all the considered structures, the band at ~ 1210 cm^{-1} does not appear in their theoretical vibrational spectra based on the harmonic approximation (Figs. S12-S13). The use of anharmonic theory is required for its correct prediction [32]. However, anharmonic calculations are not as straightforward to interpret and use for assignment purposes. Although they predict the anharmonic band at ~ 1210 cm^{-1} well, a significant shift in the fundamental bands is often observed, thereby making the interpretation of the IR spectra difficult [15]. To overcome this problem, overtones and combination bands were calculated for all the isomers by performing NEARIR calculations, as shown in Fig. 5. Other bands, mainly in the region of 800 – 1000 cm^{-1}, were not predicted in any of the calculated spectra. These missing bands could be generated by vibrational modes of other molecular species having a $m/z = 140$, which have not been considered in this work. Other isomers of $m/z = 140$, such as 2-ethynyl-1H-indene and cyclopropanaphthalene, were also considered but were discarded as possible contributors due to the absence of their most intense bands in the experimental IR spectrum (Fig. S10).

The spectrum corresponding to $m/z = 151$ was assigned to a combination of the eight isomers 2-(buta-1,3-diyn-1-yl)benzonitrile, 3-(buta-1,3-diyn-1-yl)benzonitrile, 4-(buta-1,3-diyn-1-yl)benzonitrile, 2,3-diethynylbenzonitrile, 3,4-diethynylbenzonitrile, 2,4-diethynylbenzonitrile, 2,6-diethynylbenzonitrile, and 3,5-diethynylbenzonitrile. This assignment was further confirmed by the presence of the overtone at ~ 1210 cm^{-1} in the experimental IR spectrum (Fig. 6). Similarly to the case of $m/z = 140$, this band was predicted using the NEARIR option for most of the isomers of $m/z = 151$, as shown in Fig. 6. Other species of $m/z = 151$, which could have formed upon the ring opening of

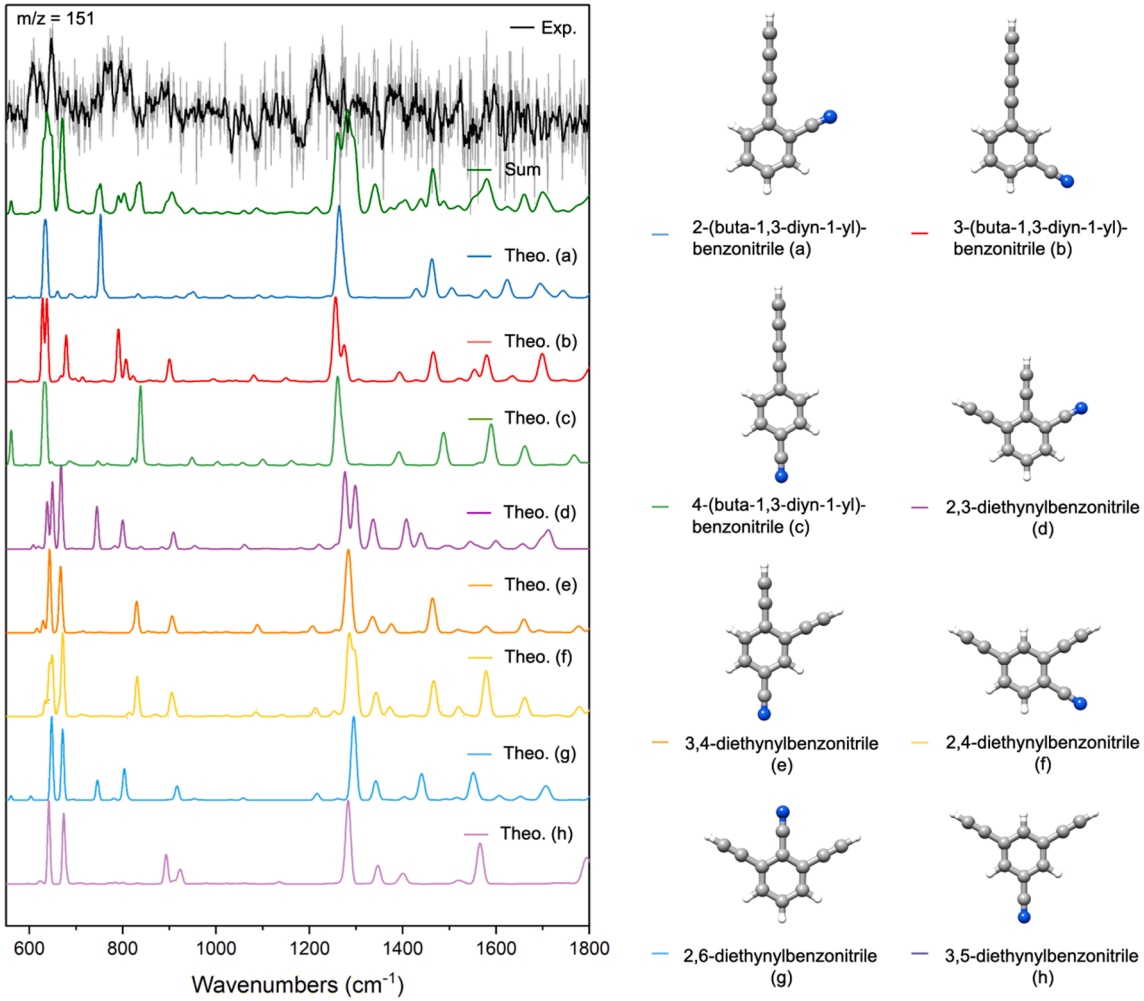

Fig. 6. Comparison of the experimental IR spectrum (black trace) recorded in the 550 – 1800 cm^{-1} frequency region for $m/z = 151$ with the theoretical NEARIR vibrational spectra calculated at the B3LYP/def2-TZVP level of theory for several isomers (left). The trace in light gray shows the average of the experimental IR spectra. The black trace represents the averaged experimental IR spectrum after applying a 5-point adjacent-average smooth function. The colored traces provide the theoretical vibrational spectra calculated for the molecular structures given on the right-hand side of the figure (a-h). A scale factor of 0.9671 was applied to the theoretical spectra.

naphthalene, such as 5-phenylpenta-2,4-diynenitrile, were also considered as possible reaction products but they were excluded due to a clear mismatch of their theoretical spectra with the experimental data (Fig. S11).

The experimental IR spectrum corresponding to $m/z = 167$ was assigned to the equatorial and axial conformers of six isomers of 7H-benzo[7]annulenecarbonitrile. The combination of their theoretical IR spectra was found to be in good agreement with the experimental data and matched the region of the experimental IR spectrum between 700 cm^{-1} and 900 cm^{-1} (Fig. 7). The experimental IR spectrum exhibits three main vibrational bands, two fall in the range ~ 710 – 740 cm^{-1} and arise from the CH out-of-plane wagging motion also involving an out-of-plane deformation of the ring, and one at ~ 800 cm^{-1}, generated by the CH out-of-plane bending motion. Due to the similarities between the calculated vibrational spectra of the six isomers of 7H-benzo[7] annulenecarbonitrile, we could not discriminate between them.

4. Discussion

In general, the outcome of a rich chemistry is observed when a mixture of naphthalene and acetonitrile undergoes electrical discharge. In the experiment of pure naphthalene [15], the formation of two types of PAHs was observed. These included larger PAHs and polyyne-substituted PAHs. With acetonitrile as an additional precursor, we can distinguish between two new classes of molecules, namely carbonitrile (–CN) and methyl ($–CH_3$) substituted aromatic rings.

The mass information provided by the technique gave important guidance to identify the different classes of molecules. Several IR spectra of a certain mass have been assigned to a combination of isomers. Although some isomers could be excluded based on a poor agreement between the calculated and experimental spectra, a unique assignment to just one particular structure proved to be particularly challenging. This is mostly due to the relatively low signal-to-noise ratio, as well as to overlapping spectral signatures of the possible isomers. From a theoretical point of view, a more detailed assignment of the spectra can be assisted by performing NEARIR calculations so that overtones and combination bands could be identified, as shown for some of the species identified in this work. From an experimental point of view, an optimization of the excitation wavelength for each identified mass channel would improve the signal-to-noise ratio of the IR spectra. Furthermore, experiments in the far-IR region would allow for the measurement of higher-resolution spectra but also IR-IR double resonance spectroscopy or microwave spectroscopy experiments would allow for an unequivocal isomeric discrimination. A quantitative analysis of the relative amounts of the observed species is complicated due to the spectral dependence on the excitation and ionization cross section of the molecular species and to the use of a single

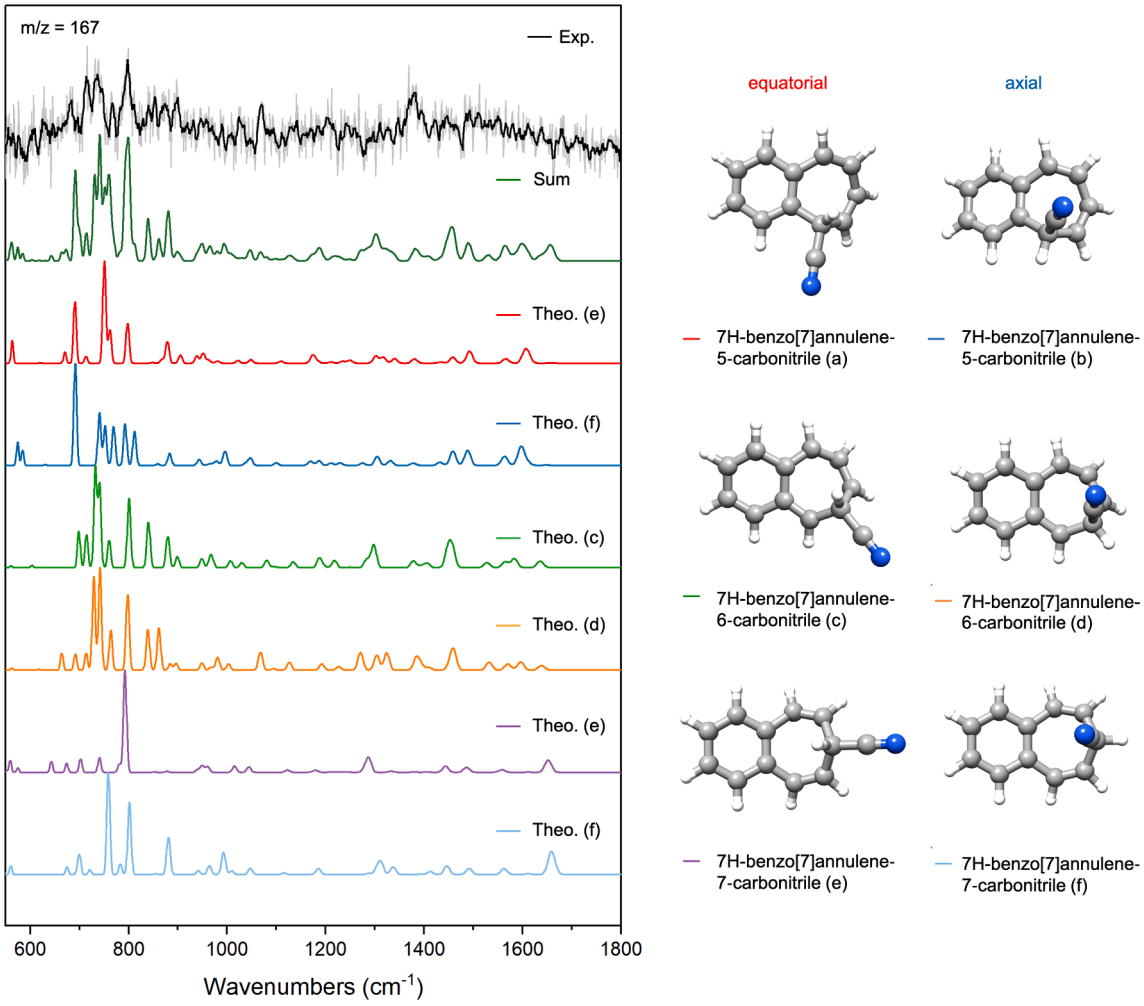

Fig. 7. Comparison of the experimental IR spectrum (black trace) recorded in the 550 – 1800 cm^{-1} frequency region for $m/z = 167$ with the theoretical vibrational spectra calculated at the B3LYP/6–31+G* level of theory for the equatorial and axial conformers of the six isomers of 7H-benzo[7]annulenecarbonitrile (colored traces). The black trace shows the experimental IR spectrum after applying a 5-point adjacent-average smooth function. The trace in light gray represents the average of the experimental IR spectra. The green trace provides the sum of the calculated spectra of the two conformers. A scale factor of 0.976 was applied to the theoretical spectra. (For interpretation of the references to color in this figure legend, the reader is referred to the web version of this article.)

excitation wavelength (275 nm) for all the mass channels; therefore, in the following, we discuss some qualitative observations.

Under the given experimental conditions, the peak at $m/z = 153$ is the most intense in the mass spectrum, and it was assigned to the two isomers 1-cyanonaphthalene and 2-cyanonaphthalene. The formation of these molecules can take place via a neutral-radical reaction between naphthalene and the radical CN [33–36]. A schematic of the potential reaction mechanism within the discharge experiments leading to the formation of cyanonaphthalene is illustrated in Fig. 8. The two isomers 1- and 2-methylnaphthalene are likely to be formed via a similar neutral-radical reaction pathway as for cyanonaphthalene (Fig. 8). However, we expect that an attempt to detect these species via radio astronomy would be challenging due to their relatively low electric dipole moments of 0.3 and 0.5 Debye for 1-methylnaphthalene and 2-methylnaphthalene, respectively, compared to dipole moments of 4.7 and 5.3 Debye calculated for 1-cyanonaphthalene and 2-cyanonaphthalene, respectively.

The peak in the mass spectrum at $m/z = 140$ was partially assigned to a series of methyl substituted diacetylenebenzene and diethynylbenzene, which could form upon the ring opening in the precursors naphthalene or methylnaphthalene. We can indeed propose two formation routes to explain the observation of some of these species, since both naphthalene ($m/z = 128$) and methylnaphthalene ($m/z = 142$) are known to be present in our experiment. If we consider 1-(buta-1,3-diyn-1-yl)-2-methylbenzene, this species could form via a two-step reaction mechanism involving first a C-C cleavage to form diacetylenebenzene, also identified as $m/z = 126$ in our experiment (Fig. S4 of the SI), and then a reaction of diacetylenebenzene with the CH_3 radical when starting with naphthalene as the precursor (Fig. 8). Alternatively, methylnaphthalene could form first, via a neutral-radical reaction between naphthalene and the CH_3 radical, to then undergo C-C rupture to produce 1-(buta-1,3-diyn-1-yl)-2-methylbenzene (Fig. 9). Since both diacetylenebenzene ($m/z = 126$) and methylnaphthalene ($m/z = 142$) have been assigned in our experiment, both proposed mechanisms should be taken into consideration.

As mentioned before, a discrimination between the species assigned to $m/z = 140$ is not possible due to their similar vibrational spectra. However, most of them have a sufficient dipole moment, thus suggesting that their unambiguous assignments could be possible by microwave spectroscopy, a spectroscopic technique which is extremely sensitive to small structural differences. A parallel study via microwave spectroscopy is underway in the Hamburg group.

A similar reaction pathway to the one for $m/z = 140$, this time involving the CN radical instead of the CH_3 radical (Fig. 8), can also explain the observation of the species having a mass-to-charge ratio of 151, which was assigned to a series of carbonitrile-substituted diethynylbenzene and diacetylenebenzene.

The six isomers of 7H-benzo[7]annulenecarbonitrile ($m/z = 167$) are thought to be the result of a radical–radical reaction occurring between the radical CN and the resonance-stabilized radical 7H-benzo[7]annulene ($m/z = 141$) (Fig. 9), which is known to form when naphthalene is subjected to electrical discharge (Fig. S5) [15].

5. Conclusions

Our experiment elucidates the chemistry that the naphthalene/acetonitrile mixture undergoes when subjected to the harsh energetic conditions generated by an electrical discharge source. In this work, among the carbon-chain-substituted aromatic molecules observed, new –CN and $–CH_3$ substituted species have been identified. Most of these species, especially those containing a nitrogen atom in their molecular structure, such as the benzo[7]annulenecarbonitrile, have substantial dipole moments and, therefore, represent good candidates for astronomical observation in interstellar regions, such as the molecular cloud TMC-1, where CN-functionalized rings, including benzonitrile, [37] 1- and 2-cyano-1,3-cyclopentadiene [38], and 1- and 2-cyanonaphthalene [6], have been already discovered.

The use of electrical discharge sources as a way of making new species has been previously shown to create astronomically relevant species [39–41]. With the observation of the two isomers of cyanonaphthalene in our experiment, we further highlight that this also holds true for PAH-like molecules, which, nowadays, represent one of the main targets of astronomical searches.

To unambiguously confirm the assignment of the observed species, we have recently investigated the electrical discharge chemistry of the naphthalene/acetonitrile mixture using microwave spectroscopy as a complementary approach. These experiments will be particularly useful to disentangle the different isomers with $m/z = 140$, 151 and 167, which will be nicely distinguishable with rotational spectroscopy because of

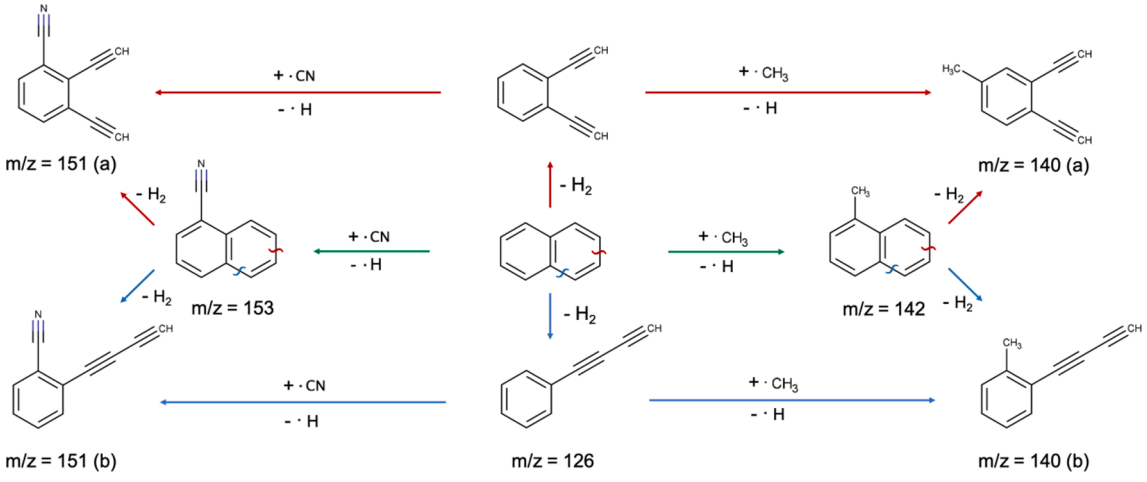

Fig. 8. Schematic of the proposed reaction mechanisms for the formation of $m/z = 140$, 142, 151 and 152. The green arrows indicate the neutral-radical reaction occurring between the precursor naphthalene and the CH_3 and CN radicals, which are generated upon discharge of acetonitrile, to form methylnaphthalene ($m/z = 142$) and cyanonaphthalene ($m/z = 153$), respectively. The red arrows indicate the mechanism starting with the C-C cleavage of the precursor naphthalene and leading to the formation of 1,2-diethynylbenzene, which in turn can react with the CH_3 and CN radicals to form $m/z = 140$ (a) and 151 (a), respectively. The blue arrows indicate the mechanism starting with the C-C cleavage of naphthalene and leading to the formation of diacetylenebenzene, which successively can react with the CH_3 and CN radicals to form $m/z = 140$ (b) and $m/z = 151$ (b), respectively. M/z = 151 can also form upon C-C cleavage of cyanonaphthalene. Similarly, $m/z = 140$ can form upon C-C cleavage of methylnaphthalene. (For interpretation of the references to color in this figure legend, the reader is referred to the web version of this article.)

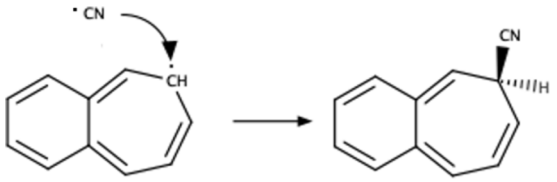

Fig. 9. Proposed radical–radical reaction mechanism between the benzo[7] annulene radical and the cyano radical leading to the formation of 7H-benzo[7] annulenecarbonitrile.

their sufficient electric dipole moments.

Author contributions

Amanda Steber, Anouk M. Rijs, and Melanie Schnell conceived and designed the experiments.

Melanie Schnell acquired the funding for the experiment.

Donatella Loru, Amanda L. Steber, Alexander K. Lemmens, Daniël B. Rap, and Johannes M. M. Thunnissen performed the experiments.

Donatella Loru, Alexander K. Lemmens, and Daniël B. Rap performed the theoretical calculations.

Donatella Loru, Alexander K. Lemmens, Daniël B. Rap, and Johannes M. M. Thunnissen worked on the data analysis.

The original draft was written by Donatella Loru.

All the authors contributed to the reviewing and editing of the manuscript.

Declaration of Competing Interest

The authors declare that they have no known competing financial interests or personal relationships that could have appeared to influence the work reported in this paper.

Acknowledgments

This work was supported via the ERC starting grant 'ASTROROT' (grant number 638027). D.L. was supported by a Alexander von Humboldt postdoctoral fellowship. We would like to thank the FELIX laboratory team for their experimental assistance, and we acknowledge the Nederlandse Organisatie voor Wetenschappelijk Onderzoek (NWO) for the support of the FELIX laboratory. The research leading to this result has been supported by the project CALIPSOplus under the Grant Agreement 730872 from the EU Framework Programme for Research and Innovation HORIZON 2020.

Appendix A. Supplementary data

Supplementary data to this article can be found online at https://doi.org/10.1016/j.jms.2022.111629.

References

[1] L.J. Allamandola, A.G.G.M. Tielens, J.R. Barker, The Astrophys. J. Supplement Series 71 (1989) 733.
[2] A.G.G.M. Tielens, EAS Publications Series 46 (2011) 3–10.
[3] A.G.G.M. Tielens, Ann. Rev. Astron. Astrophys. 46 (2008) 289–337.
[4] J. Cernicharo, M. Agúndez, C. Cabezas, B. Tercero, N. Marcelino, J.R. Pardo, P. de Vicente, A&A 649 (2021) L15.
[5] A.M. Burkhardt, K.L.K. Lee, P.B. Changala, C.N. Shingledecker, I.R. Cooke, R. A. Loomis, H. Wei, S.B. Charnley, E. Herbst, M.C. McCarthy, B.A. McGuire, ApJL 913 (2021) L18.
[6] B.A. McGuire, R.A. Loomis, A.M. Burkhardt, K.L.K. Lee, C.N. Shingledecker, S. B. Charnley, I.R. Cooke, M.A. Cordiner, E. Herbst, S. Kalenskii, M.A. Siebert, E. R. Willis, C. Xue, A.J. Remijan, M.C. McCarthy, Science 371 (2021) 1265–1269.
[7] J. Zhen, P. Castellanos, D.M. Paardekooper, H. Linnartz, A.G.G.M. Tielens, Astrophys J 797 (2014) L30.
[8] O. Berné, J. Montillaud, C. Joblin, A&A 577 (2015) A133.
[9] P. Merino, M. Švec, J.I. Martinez, P. Jelinek, P. Lacovig, M. Dalmiglio, S. Lizzit, P. Soukiassian, J. Cernicharo, J.A. Martin-Gago, Nat Commun 5 (2014) 3054.
[10] B. Shukla, M. Koshi, Combust. Flame 159 (2012) 3589–3596.
[11] E. Reizer, B. Viskolcz, B. Fiser, Chemosphere (2021), 132793.
[12] P.M. Woods, T.J. Millar, A.A Zijlstra, E. Herbst, The Astrophysical Journal 574 (2002) L167–L170.
[13] B.M. Jones, F. Zhang, R.I. Kaiser, A. Jamal, A.M. Mebel, M.A. Cordiner, S. B. Charnley, PNAS 108 (2010) 452–457.
[14] A.M. Rijs, M. Kabeláč, A. Abo-Riziq, P. Hobza, M.S. de Vries, ChemPhysChem 12 (2011) 1816–1821.
[15] A.K. Lemmens, D.B. Rap, J.M.M. Thunnissen, B. Willemsen, A.M. Rijs, Nat. Commun. 11 (2020) 269.
[16] A.J. Remijan, J.M. Hollis, F.J. Lovas, D.F. Plusquellic, P.R. Jewell, ApJ 632 (2005) 333.
[17] K.I. Öberg, V.V. Guzmán, K. Furuya, C. Qi, Y. Aikawa, S.M. Andrews, R. Loomis, D. J. Wilner, Nature 520 (2015) 198–201.
[18] Y.C. Minh, W.M. Irvine, M. Ohishi, S. Ishikawa, S. Saito, N. Kaifu, Astron. Astrophys. 267 (1993) 229–232.
[19] T. Streibel, R. Zimmermann, Annu. Rev. Anal. Chem. (Palo Alto Calif) 7 (2014) 361–381.
[20] F. Hirsch, P. Constantinidis, I. Fischer, S. Bakels, A.M. Rijs, Chem. – A Eur. J 24 (2018) 7647–7652.
[21] D. Oepts, A.F.G. van der Meer, P.W. van Amersfoort, Infrared Phys. Technol. 36 (1995) 297–308.
[22] A.D. Becke, J. Chem. Phys. 98 (1993) 5648–5652.
[23] C. Lee, W. Yang, R.G. Parr, Phys. Rev. B 37 (1988) 785–789.
[24] M.J.G. Frisch, et al., Gaussian 16, Revision A.03, Gaussian, Inc., Wallingford CT, 2016.
[25] F. Neese, WIREs Comput. Mol. Sci. 2 (2012) 73–78.
[26] F. Neese, WIREs Computational Molecular Science, 2018, 8, e1327.
[27] M.K. Kesharwani, B. Brauer, J.M.L. Martin, J. Phys. Chem. A 119 (2015) 1701–1714.
[28] P. Li, W.Y. Fan, J. Appl. Phys. 93 (2003) 9497–9502.
[29] P.J. Linstrom, W.G. Mallard, J. Chem. Eng. Data 46 (2001) 1059–1063.
[30] R.A. Nyquist, W.J. Potts, Spectrochim. Acta 16 (1960) 419–427.
[31] J.C. Evans, R.A. Nyquist, Spectrochim. Acta 19 (1963) 1153–1163.
[32] P. Constantinidis, F. Hirsch, I. Fischer, A. Dey, A.M. Rijs, J. Phys. Chem. A 121 (2017) 181–191.
[33] N. Balucani, O. Asvany, A. Chang, S.-Z. Lin, Y. Lee, R. Kaiser, H. Bettinger, P. Schleyer, H. Schaefer, J. Chem. Phys 111 (1999) 7457–7471.
[34] C.J. Bennett, S.B. Morales, S.D.L. Picard, A. Canosa, I.R. Sims, Y.H. Shih, A.H. H. Chang, X. Gu, F. Zhang, R.I. Kaiser, Phys. Chem. Chem. Phys. 12 (2010) 8737–8749.
[35] I.R. Cooke, D. Gupta, J.P. Messinger, I.R. Sims, ApJL 891 (2020) L41.
[36] K.L.K. Lee, B.A. McGuire, M.C. McCarthy, Phys. Chem. Chem. Phys. 21 (2019) 2946–2956.
[37] B.A. McGuire, A.M. Burkhardt, S. Kalenskii, C.N. Shingledecker, A.J. Remijan, E. Herbst, M.C. McCarthy, Science 359 (2018) 202–205.
[38] M.C. McCarthy, K.L.K. Lee, R.A. Loomis, A.M. Burkhardt, C.N. Shingledecker, S. B. Charnley, M.A. Cordiner, E. Herbst, S. Kalenskii, E.R. Willis, C. Xue, A. J. Remijan, B.A. McGuire, Nat. Astron. 5 (2021) 176–180.
[39] M.C. McCarthy, W. Chen, M.J. Travers, P. Thaddeus, The Astrophys. J. Supplement Series 129 (2000) 611–623.
[40] M.C. McCarthy, E.S. Levine, A.J. Apponi, P. Thaddeus, J. Mol. Spectrosc. 203 (2000) 75–81.
[41] M.C. McCarthy, K.L.K. Lee, P.B. Carroll, J.P. Porterfield, P.B. Changala, J. H. Thorpe, J.F. Stanton, J. Phys. Chem. A 124 (2020) 5170–5181.